Published in final edited form as:
FEMS Microbiol Lett. 2009 January ; 290(2): 164–173. doi:10.1111/j.1574-6968.2008.01416.x.

Transcription and genetic analyses of a putative *N*-acetylmuramyl-L-alanine amidase in *Borrelia burgdorferi*

Yu Yang and **Chunhao Li**
Department of Oral Biology, State University of New York at Buffalo, NY, USA

Abstract

In this study, a putative *N*-acetylmuramyl-L-alanine amidase gene (*bb0666*) was identified in the genome of the Lyme disease spirochete *Borrelia burgdorferi*. This protein shares *c.* 30% identity with its counterparts from other bacteria. Reverse transcriptase-PCR analysis showed that *bb0666* along with two other genes (*bb0665* and *bb0667*) are cotranscribed with the motility and chemotaxis genes. This newly identified operon is termed as *pami*. Sequence and primer extension analyses showed that *pami* was regulated by a σ^{70}-like promoter, which is designated as P_{ami}. Transcriptional analysis using a gene encoding green fluorescence protein as a reporter demonstrated that P_{ami} functions in both *Escherichia coli* and *B. burgdorferi*. Genetic studies showed that the Δ*bb0666* mutant grows in long chains of unseparated cells, whose phenotype is similar to its counterparts in *E. coli*. Taken together, these results demonstrate that *bb0666* is a homolog of MurNac-LAAs that contributes to the cell division of *B. burgdorferi*.

Keywords

lyme disease; *Borrelia burgdorferi*; *N*-acetylmuramyl-L-alanine amidase

Introduction

Spirochetes are a medically significant but poorly understood group of bacteria. These organisms cause several human diseases such as syphilis, Lyme disease and leptospirosis (Charon & Goldstein, 2002). Spirochetes constitute a very diverse but monophyletic group of bacteria that have common morphological and structural attributes (Paster & Dewhirst, 2000). Compared with other bacterial species, the morphology of spirochete cells is quite unique (Li *et al.*, 2000; Charon & Goldstein, 2002). They are either wave-like or helical, and the average size of spirochete cells is *c.* 10–20 μm in length and 0.1–0.3 μm in width, which is much slimmer than other bacterial species such as *cocci*- or *bacilli*-shaped bacteria. In addition, spirochetes share a unique cell structure: a protoplasmic cell cylinder surrounded by an outer membrane sheath. In the periplasm, between the peptidoglycan layer and the outer membrane sheath are periplasmic flagella (PF) that are attached at both ends of the cell (Charon & Goldstein, 2002; Limberger, 2004). Because of a paucity of genetic tools and their fastidious growth requirements, the basic biology of spirochetes is poorly understood (e.g. the molecular mechanisms of cell division and morphogenesis in spirochetes still remain unknown).

Correspondence: Chunhao Li, Department of Oral Biology, State University of New York at Buffalo, 3435 Main Street, Buffalo, NY 14214-3092, USA. Tel.: +1 716 829 6014; fax: +1 716 829 3942; cli9@buffalo.edu.

Cell division is an essential biological process for the growth and survival of bacterial cells (Margolin, 2006; Barak & Wilkinson, 2007; Lock & Harry, 2008). The molecular mechanisms involved in cell division have been most extensively studied in rod-shaped bacteria (*Escherichia coli* and *Bacillus subtilis*) (Barak & Wilkinson, 2007; Lutkenhaus, 2007). In these model organisms, cell division initiates from the formation of a Z-ring that occurs at the center of the cell. Following the formation of a Z-ring, the membrane-bound cell division proteins are recruited, resulting in the invagination of the cell wall and membrane to form a division septum. Once septum formation is complete, the peptidoglycan layer in the division septum is cleaved by specific peptidoglycan hydrolases, allowing two newborn cells to separate (Holtje & Heidrich, 2001; Vollmer *et al.*, 2008). Bacterial peptidoglycan hydrolases form a vast and highly diverse group of enzymes that are capable of cleaving bonds in polymeric peptidoglycan. Among these enzymes, *N*-acetylmuramyl-L-alanine amidases (MurNac-LAAs) specifically hydrolyze the amide bond between *N*-acetylmuramic acid and the N-terminal L-alanine residue of the stem peptide (Holtje & Heidrich, 2001; Vollmer *et al.*, 2008).

In *E. coli*, there are five amidases (AmiA, B, C, D and AmpD). Based on their sequence differences, these amidases can be divided into two groups (Bernhardt & de Boer, 2003; Vollmer *et al.*, 2008). The first group is composed of AmiA, B and C enzymes, and the second contains AmiD and AmpD. The functions, enzymatic activity and cellular location of the first group are well studied (Heidrich *et al.*, 2001; Bernhardt & de Boer, 2003). Genetic studies have shown that the deletion mutants in *amiA* and *amiC* grow in long chains of unseparated cells, indicating that these two amidases play an important role in cleaving the septum to release daughter cells after cell division (Heidrich *et al.*, 2001; Bernhardt & de Boer, 2003). In contrast to *E. coli*, there is only one putative MurNac-LAA gene annotated in the sequenced spirochete genomes (*bb0625* in *Borrelia burgdorferi*, *TDE1714* in *Treponema denticola*, *TP0247* in *Treponema pallidum* and *LA3433* in *Leptospira interrogans*) (Fraser *et al.*, 1997, 1998; Ren *et al.*, 2003; Seshadri *et al.*, 2004). The function of these genes in spirochetes remains unknown. *Borrelia burgdorferi* is the causative agent of Lyme disease, the most commonly reported tick-borne disease in the United States (Steere, 2001; Kurtenbach *et al.*, 2006). In addition to being an important clinical entity, *B. burgdorferi* is one of the best understood spirochetes and one for which genetic tools have rapidly evolved in the past few years (Rosa *et al.*, 2005), making it currently an ideal genetic model to investigate the role of MurNac-LAAs. In the present study, we report that an unannotated MurNac-LAA homolog (*bb0666*) contributes to the cell division of *B. burgdorferi*. This finding provided us with a starting point to further elucidate the roles of MurNac-LAAs in the cell division of *B. burgdorferi* and other spirochete species.

Materials and methods

Bacterial strains and growth conditions

A high-passage avirulent *B. burgdorferi* strain (B31A) was used as a parental strain to perform the transcriptional and genetic studies of *bb0666* (Motaleb *et al.*, 2000; Li *et al.*, 2002; Sal *et al.*, 2008). B31A and its derived strains were grown in Barbour–Stoenner–Kelly (BSK)-II liquid medium or on plates with or without kanamycin (300 μg mL^{-1}) or streptomycin (80 μg mL^{-1}) at 34 °C in 3% carbon dioxide as described before (Li *et al.*, 2002; Sal *et al.*, 2008). *Escherichia coli* strain JM109 (Promega) was used for plasmid construction, amplification and expression of the *gfp* gene. *Escherichia coli* strain M15 (Qiagen) was used for the preparation of the recombinant BB0666 protein.

PCR, reverse transcriptase (RT)-PCR and primer extension analyses

These analyses were performed as described previously (Ge *et al.*, 1997a, b). All the primers used for PCR, RT-PCR and primer extension analyses are listed in Table 1. For PCR, either Taq (Invitrogen) or Vent (New England Biolabs) DNA polymerases were used. For RNA isolation, 100 mL of mid-exponential-phase *B. burgdorferi* cells were harvested and washed twice with cold phosphate-buffered saline (pH 8.0). Total RNA was isolated with Tris Reagent (Sigma-Aldrich) according to the manufacturer's instructions, followed by a treatment with RNAse-free DNAse I (Promega). Further purification of RNA samples was performed using a Qiagen RNA isolation kit. The AMV Reverse Transcriptase Primer Extension System (Promega) was used to generate cDNA for RT-PCR or for primer extension analysis.

Primer extension analysis was performed as before with slight modification (Ge *et al.*, 1997a, b). Briefly, 20 pmol of the primer *P15* (Table 1) was labeled with ^{32}P-ATP at 37 °C for 30 min and purified with a Qiagen Nucleotide Removal Kit. For reverse transcription, 1 μL of labeled primer was mixed with 20 μg RNA and incubated at 58 °C for 20 min. AMV reverse transcriptase and other reagents were then added, and the extension reaction was carried out at 42 °C for 45 min. The resultant cDNA products were precipitated with ethanol and dissolved in 5 μL standard DNA loading buffer. The obtained samples, along with an ^{35}S-labeled DNA ladder, which was generated from sequencing the *B. burgdorferi flaA* gene, were separated on a 6% polyacrylamide–8M urea denaturing gel. The gels were dried and analyzed on a PhosphorImager system (Storm 860, Molecular Dynamics). The identified promoter consensus was designated P_{ami}.

Fluorescent reporter constructs

To test whether P_{ami} was functional, a mutant *gfp* gene was used as a transcriptional reporter (Eggers *et al.*, 2002). In addition, previously identified *flaA*, *flaB* and *flgB* promoters (P_{flaA}, P_{flaB} and P_{flgB}, respectively) were used as controls to evaluate the strength of P_{ami} (Ge & Charon, 1997a; Ge *et al.*, 1997a, b). To fuse P_{ami} to *gfp*, the fragment containing P_{ami} was PCR amplified using primers *P24/P25* with engineered PstI and BamHI restriction cut sites at the 5′ and 3′ ends, respectively. The obtained PCR product was then cloned into the pGEM-T Easy vector (Promega). Meanwhile, the full-length *gfp* gene was PCR amplified with engineered BamHI and PstI restriction at 5′ and 3′ ends, respectively. The *gfp* gene was fused to P_{ami} at the BamHI cut site by restriction digestion and religation. The fused P_{ami}-*gfp* fragment was digested with PstI and further cloned into the shuttle vector pKFSS1 (Frank *et al.*, 2003), creating the vector P_{ami}-*gfp*/pKFSS1. The same method was used to fuse other promoters to *gfp*, and created vectors P_{flaA}-*gfp*/pKFSS1, P_{flaB}-*gfp*/pKFSS1 and P_{flgB}-*gfp*/pKFSS1. These vectors were, respectively, transformed into either *E. coli* strain JM109 or *B. burgdorferi* strain B31A to monitor the expression level of green fluorescence protein (GFP). The expression of GFP was visualized with fluorescent microscopy (Axiostar Plus, Ziess), and the levels of GFP in transformed strains were evaluated by either Western blot using a monoclonal GFP antibody (Invitrogen) or a fluorometer model LPS-220B at excitation wavelength 494 nm (Photon Technology International Inc.).

Preparation of recombinant BB0666 and antiserum against BB0666

The full-length *bb0666* gene was PCR amplified using primers *P5/P6* with engineered BamHI and PstI cut sites at the 5′ and 3′ ends, respectively. The obtained PCR product was then cloned into the BamHI–PstI-restricted pQE30 vector (Qiagen), which expresses a six-histidine tag at the N-terminus of the recombinant protein. The overexpression of *bb0666* was induced with 1 mM isopropyl-β-D-thiogalactoside. His-tagged BB0666 was purified with nickel agarose columns and concentrated in 10-kDa molecular weight cut-off Amicon ultracentrifugal concentrators (Millipore). To raise the antiserum against BB0666, rabbits

were immunized with 400μg of purified recombinant protein over 1 month. Polyclonal antiserum was further purified with a Protein A IgG Purification Kit (Pierce).

Construction of the *bb0666* deletion mutant and complementation of the mutant

Similar methods described before were used to inactivate the *bb0666* gene (Motaleb *et al.*, 2000; Li *et al.*, 2002; Sal *et al.*, 2008). As described in Fig. 1, the DNA fragment containing *bb0666* was PCR amplified and the obtained PCR product was cloned into the pGEM-T Easy vector, yielding pbb0666-Easy. Meanwhile, a kanamycin-resistance marker (*kan*) described before (Bono *et al.*, 2000) was PCR amplified to engineer HindIII (5′) and MunI (3′) restriction sites. A 96-bp HindIII–MunI fragment within *bb0666* was deleted and replaced with *kan*, creating the vector pbb0666::kan. This plasmid was linearized and transformed into B31A strain by electroporation as described before (Samuels, 1995). Transformants were selected on soft BSK-II agar containing 300 μg mL^{-1} kanamycin. The targeted mutagenesis was confirmed by PCR and the loss of the cognate gene product was detected by Western blot as described before (Motaleb *et al.*, 2000; Li *et al.*, 2002; Sal *et al.*, 2008). The obtained mutant was designated as Δ*bb0666*.

To complement Δ*bb0666*, the entire length of *bb0666* was PCR amplified, and the resultant product was fused to P_{flgB} at an NdeI site and the resultant P_{flgB}-*bb0666* fragment was further cloned into the shuttle vector pKFSS1 at BamHI and PstI sites, creating the complemented vector, FlgB666/pKFSS1 (Fig. 1b). To complement Δ*bb0666*, the vector FlgB666/pKFSS1 was transformed into the mutant cells by electroporation. The selection and characterization of the complemented mutant was performed as described previously. The obtained mutant was referred to as Δ$bb0666^{+}$.

Gel electrophoresis and Western blot analysis

Sodium dodecyl sulfate-polyacrylamide gel electrophoresis (SDS-PAGE) and Western blotting with an enhanced chemiluminescent detection method (ECL-Amersham Pharmacia) were carried out as reported previously (Motaleb *et al.*, 2004; Sal *et al.*, 2008). The concentration of cellular proteins in lysates was determined by a Bio-Rad protein assay kit. Ten micrograms of whole cell lysates were run by SDS-PAGE and were subjected to Western blot using specific antibodies. For quantitative Western blot, the *B. burgdorferi* flagella filament protein, FlaB, and *E. coli* flagella motor switch protein, FliG, were used as internal controls. Monoclonal antibody against FlaB (H9724) and polyclonal antibody against FliG were kindly provided by A.G. Barbour (University of California, Irvine) and R. Macnab (Yale University), respectively. The monoclonal antibody against GFP was purchased from Invitrogen. The amounts of immunoreactive proteins in the gels were determined using FluorChem spot densitometry as before (Motaleb *et al.*, 2004; Sal *et al.*, 2008).

Light and electron microscopy

The mutant and complemented strains were visually examined under dark-field microscope for altered cell morphology. The images were captured and processed with the software AXIOVISION AC 4.1 (Zeiss). The membrane-disrupted cells were prepared and visualized under an electron microscope as described before (Motaleb *et al.*, 2000; Li *et al.*, 2002; Sal *et al.*, 2008).

Results

BB0666 is a homolog of MurNac-LAAs

The genes encoding MurNac-LAAs are widely distributed among bacteria, and many bacterial species contain multiple MurNac-LAAs (Heidrich *et al.*, 2002; Kajimura *et al.*,

2005; Vollmer *et al.*, 2008). For instance, *E. coli* has five MurNac-LAAs (Heidrich *et al.*, 2001; Bernhardt & de Boer, 2003). In contrast, only one MurNac-LAA homolog (BB0625) was annotated in the genome of *B. burgdorferi* (Fraser *et al.*, 1997). To detect whether there are other potential MurNac-LAA homologs, the *E. coli* MurNac-LAAs were used as queries to search the genome of *B. burgdorferi*. From these searches, BB0666 was found to have significant similarity to AmiA, B and C (*e*-values < 10^{-7}). In contrast, a previously annotated putative MurNac-LAA (BB0625) showed less similarity to the *E. coli* MurNac-LAAs (*e*-values > 0.05), indicating that BB0666 is likely a homolog of MurNac-LAA, but BB0625 is not.

BB0666 consists of 342 amino acids and its predicted molecular weight is *c*. 40 kDa. To further confirm whether this protein belongs to the family of MurNac-LAAs, BB0666 was used to query the database of Pfam (http://pfam.sanger.ac.uk), and the results show that BB0666 belongs to the family of amidase_3 (PF01520) (*e*-values < 10^{-40}). The C-terminus (118–335 amino acids) of BB0666 contains a well-conserved catalytic domain that is present in MurNac-LAAs from a variety of different bacteria (Fig. 2) (Shida *et al.*, 2001;Mishima *et al.*, 2005). Sequence alignment analyses further revealed that some residues within the catalytic domains are well conserved among different bacterial species. Genetic and biochemical studies of CwlC, a MurNac-LAA of *B. subtilis*, indicate that some of those conserved residues are essential for the enzymatic activity of CwlC. For example, the substitution of residues E24, D55, H79 and E141 completely abolished the activity of CwlC (Shida *et al.*, 2001). Consistently, those four residues are well conserved in BB0666 and other MurNac-LAAs (Fig. 2). Taken together, these results have suggested that BB0666 is most likely a MurNac-LAA that is involved in the cleavage of peptidoglycan during the cell division of *B. burgdorferi*.

The *bb0666* gene is cotranscribed with the genes of the *flaA* operon

The two genes adjacent to *bb0666* (*bb0665* and *bb0667*; Fig. 3a) encode two conserved hypothetical proteins (Fraser *et al.*, 1997), and these three genes are adjacent to a previously identified *flaA* operon (Ge & Charon, 1997a,b). There is only 71 bp of intergenic space between *bb0667* and the *flaA* gene (*bb0668*) (Fraser *et al.*, 1997). In addition, the ORFs encoding these genes reside on the same DNA strand as the genes of the *flaA* operon (Fig. 3a) (Fraser *et al.*, 1997), implying that these three genes may be cotranscribed with the *flaA* operon. To test this hypothesis, a previously described RT-PCR analysis was performed (Ge *et al.*, 1997a,b). As shown in Fig. 3a, four pairs of primers from adjacent genes spanning *bb0664* to *flaA* (*bb0668*) region were used for the RT-PCR analysis. As expected, no product was detected between *bb0664* and *bb0665* genes because they are divergently transcribed. In contrast, all other primers yielded PCR products of predicted sizes (Fig. 3b). These results indicate that *bb0665*, *bb0666* and *bb0667* are cotranscribed with the genes of the *flaA* operon, thus constituting an eight-gene operon that is *c*. 9 kb long (Fraser *et al.*, 1997). Because *bb0666* is a homolog of *E. coli amiA*, *B* and *C* (*ami*), this newly identified operon is designated as *pami*.

The *pami* operon is initiated by a σ^{70}-like promoter

There is a 726-bp intergenic space upstream of *bb0665* (Fraser *et al.*, 1997). To understand the genetic regulation of *pami*, this region was searched for different promoter consensus sequences that typically exist in *B. burgdorferi* (e.g. σ^{70}- and σ^{54}-like promoters). A highly conserved σ^{70}-like promoter was found upstream of *bb0665*: a −10 region showing 100% identity to the consensus sequence (TATAAT), with a less-conserved −35 region (TTGTAT) (Fig. 4b) (Ge *et al.*, 1997a, b). To further confirm that transcription of *pami* is initiated from this putative promoter, a primer extension analysis was performed. As expected, the transcriptional initiation site is 7 bp downstream of the −10 region and 21 bp

from the start codon of *bb0665* (Fig. 4). Sequence comparison showed that this promoter is very similar to other σ^{70}-like promoters identified in *B. burgdorferi* (e.g. *flgB* and *flgK* promoters: their −10 regions are 100% identical; Fig. 4b) (Ge *et al.*, 1997a, b). Taken together, these results show that the identified promoter is a σ^{70}-like promoter, which is referred to as P_{ami}.

Transcriptional analysis of P_{ami} in *E. coli* and *B. burgdorferi*

To examine whether P_{ami} functions in *E. coli* and *B. burgdorferi*, the *gfp* gene was used as a transcriptional reporter as described previously (Carroll *et al.*, 2003; Eggers *et al.*, 2006). We found that both *E. coli* and *B. burgdorferi* cells harboring the vector P_{ami}-*gfp*/pKFSS1 expressed GFP protein (Fig. 5) and were fluorescent (data not shown), indicating that this promoter is functional in both *E. coli* and *B. burgdorferi*. As shown in Fig. 4, several σ^{70}-like promoters have been identified in *B. burgdorferi*, and some of these promoters (e.g. P_{flaB} and P_{flgB}) have been well characterized and used to initiate the expression of antibiotic resistance and *gfp* genes, as well as to complement mutated genes (Ge *et al.*, 1997b; Bono *et al.*, 2000; Eggers *et al.*, 2002; Carroll *et al.*, 2003). To further understand the function of P_{ami}, the strength of this promoter was compared with other σ^{70}-like promoters such as P_{flaB}, P_{flgB} and P_{flaA}. The promoter P_{flaA} is located immediately upstream of the *flaA* gene (*bb0668*). However, a previous study using the chloramphenicol-resistance marker (*cat*) as a report showed that P_{flaA} failed to express CAT in *E. coli* (Ge & Charon, 1997a; Ge *et al.*, 1997a, b). These three promoters were used as controls to evaluate the strength of the newly identified P_{ami} promoter.

Promoter activities were evaluated by measuring the level of GFP protein expressed in the transformed cells or the fluorescent intensities of the transformed cells. As shown in Fig. 5, P_{flaA} failed to express the *gfp* gene in both *E. coli* and *B. burgdorferi*, which is consistent with the previous analysis, suggesting that P_{flaA} may be a pseudo- or conditional promoter that only functions at a certain stage (e.g. within a tick or mammalian host) during the life cycle of *B. burgdorferi* (Ge *et al.*, 1997). The remaining three promoters are functional in both *E. coli* and *B. burgdorferi* (Fig. 5). Based on the levels of GFP expressed in the transformed cells, the activity of P_{flaB} is the strongest, P_{ami} is the weakest and P_{flgB} is intermediate. The ratio between these three promoters (P_{flaB} : P_{flgB} : P_{ami}) is *c.* 3 : 2 : 1 in both *E. coli* and *B. burgdorferi* (Fig. 5). A similar pattern was observed by comparing the fluorescent intensities of transformed cells (data not shown).

Inactivation of *bb0666* represses the cell division of *B. burgdorferi*

In *E. coli*, the deletion mutants in *amiA* and *amiC* grow in long chains of unseparated cells (Tomioka *et al*., 1983; Heidrich *et al*., 2001; Bernhardt & de Boer, 2003). To determine whether *bb0666* has a function similar to its counterparts in *E. coli*, the gene was inactivated as described previously (Motaleb *et al*., 2000; Li *et al*., 2002). PCR analysis demonstrated that Δ*bb0666* contained the *kan* insert as expected (data not shown), and Western blot analysis showed that the cognate gene product was absent in the mutant (Fig. 6). These results show that *bb0666* is expressed in the wild type, but is abrogated in the mutant. Microscopic analysis showed that the mutant grew in chains of multiple cells (Fig. 7), and such a phenotype was most pronounced in the stationary phase (Table 2). For example, in the early log phase, <6% of the mutant cells grew in chains (≥3 cells per chain), and this percentage was increased to *c*. 80% in the stationary phase. In contrast, <2% of the wild-type cells grow in chains (≥3 cells per chain). Electron microscopic analysis showed that the division septum was still formed between individual daughter cells (data not shown). This phenotype suggests that although the division septum can be formed in the mutant, it cannot be separated due to the inactivation of *bb0666*. A similar phenotype was observed in the *E.*

coli amiA and *amiC* mutants (*ami*-) (Tomioka *et al*., 1983; Heidrich *et al*., 2001; Bernhardt & de Boer, 2003).

Because there are several genes downstream of *bb0666*, the insertion of *kan* in the mutant may repress the expression of these genes, and the observed phenotype may be the result of a polar effect on other genes (Fraser *et al*., 1997; Ge & Charon, 1997b). To exclude this possibility, the mutant was complemented in *trans*- using the vector pBB0666/pKFSS1 (Fig. 1). The complementation successfully restored the expression of *bb0666* (Fig. 6), and the process of separating daughter cells was rescued in the complemented strain Δ*bb0666*$^{+}$ (Fig. 7). Taken together, these results have shown that *bb0666* contributes to the cell division of *B. burgdorferi*.

Discussion

Peptidoglycan hydrolyases, including MurNac-LAAs, are potentially lethal enzymes capable of disrupting bacterial cell walls. Some of these enzymes are autolysins, which are involved in programmed bacterial cell death (Holtje & Heidrich, 2001; Rice & Bayles, 2003; Vollmer *et al*., 2008). Thus, these enzymes must be highly regulated to prevent adventitious cell lysis. This regulation occurs at multiple levels from the transcriptional to the posttranslational level (Vollmer *et al*., 2008). In *B. subtilis*, the expression of *lytC* and *lytD*, which encode two amidases, is coregulated with flagellation and chemotaxis (Blackman *et al*., 1998; Serizawa *et al*., 2004). The expression of these two genes is regulated by σ^{D}, a homologof σ^{28} factors that are responsible for transcription of the genes involved in flagella assembly, motility and chemotaxis in *E. coli* and other bacteria (Hughes *et al*., 1993; Hughes & Mathee, 1998). In this report, we demonstrate that the *bb0666* gene is cotranscribed with the *flaA* operon (Fig. 3), which includes a flagella filament gene (*flaA*) and four chemotaxis genes (*cheA2, cheW3, cheX* and *cheY3*).

In many flagellated bacteria, the expression of flagellin and chemotaxis genes is regulated by σ^{28} and anti-σ^{28} factors (Aldridge & Hughes, 2002; Aldridge *et al*., 2006). However, the regulation of flagellation and chemotaxis is quite unique in *B. burgdorferi*, because σ^{28} and anti-σ^{28} factors are absent in the genome of *B. burgdorferi* (Fraser *et al*., 1997). All motility and chemotaxis genes so far identified are regulated by σ^{70} (a homolog of σ^{A}, the major housekeeping σ factor of *B. subtilis*) (Li *et al*., 2000; Charon & Goldstein, 2002). This study shows that the newly identified *pami* operon is also regulated by σ^{70} (Fig. 3). This is consistent with our previous studies (Charon & Goldstein, 2002), but differs from the regulation of *lytC* and *lytD* in *B. subtilis*, which is regulated by σ^{D} (Blackman *et al*., 1998; Serizawa *et al*., 2004). These results suggest that the coregulation between cell division and flagella formation also exists in *B. burgdorferi*. The advantage of such coregulation may allow bacterial cells to simultaneously cleave the chain between daughters, break up into single cells and swim efficiently after the flagella formation is completed. Consistent with this assumption, the *lytC* and *lytD* mutants of *B. subtilis* are unable to effectively execute swarming motility and chemotaxis due to the so-called pushmi-pullyu effect in unseparated cells (Blackman *et al*., 1998).

In *E. coli*, AmiA, B and C cleave the amide bond between Mur*N*Ac and the N-terminal L-alanine residue of the stem peptide, and they are involved in the splitting of the murein septum during cell division (Heidrich *et al*., 2001; Bernhardt & de Boer, 2003). Inactivation of *amiA* or *amiC* partially represses cell division (<30% of mutant cells grow in chains). Inactivation of *amiB* does not influence cell division. However, up to 40% of the double-mutant (with each possible combination) cells grow in chains, and up to 90% of triple-mutant cells grow in chains (Heidrich *et al*., 2001, 2002). Because cell division is an essential biological process for the growth and survival of bacterial cells, such redundancy

might be able to secure cell division. Although the cell division is significantly repressed in Δ*bb0666* (Table 2), the mutant is still able to divide at a very slow rate, indicating that there may be another peptidoglycan hydrolyase in *B. burgdorferi*.

Previous studies have shown that lytic transglycosylases (e.g. Slt70 of *E. coli*, and LytC and LytD of *B. subtilis*) are exoglucosidases that are able to degrade murein strands and contribute to bacterial cell division (Heidrich *et al*., 2001, 2002; Powell *et al*., 2006). BLAST analysis revealed that there is a lytic transglycosylase homolog (bb0625) in the genome of *B. burgdorferi*. This gene was previously annotated as a putative MurNac-LAA (Fraser *et al*., 1997). However, BLAST analysis showed that BB0625 shares little similarity with the *E. coli* MurNac-LAAs (*e*-values > 0.05). Instead, it contains multiple lysin domains (data not shown). The lysin domain is typically found in lytic transglycosylases (e.g. Slt70 of *E. coli*, and LytC and LytD of *B. subtilis*) (van Asselt *et al*., 1999; Powell *et al*., 2006). Taken together, these results suggest that BB0625 is most likely a homolog of lytic transglycosylases but not MurNac-LAAs. Thus, the remaining cell division observed in Δ*bb0666* could be due to the presence of this enzyme. Further genetic studies will help us to clarify the role of *bb0625* in *B. burgdorferi* (e.g. constructing double mutations in *bb0625* and *bb0666*).

Biochemical analyses show that the *E. coli* AmiA and C are able to cleave the amide bond between Mur*N*Ac and the N-terminal L-alanine residue of the stem peptide (Heidrich *et al*., 2001; Bernhardt & de Boer, 2003). The Δ*bb0666* mutant has a phenotype similar to the *ami*- mutants of *E. coli*, implying that BB0666 probably belongs to the family of MurNac-LAAs (Heidrich *et al*., 2001; Bernhardt & de Boer, 2003). To further confirm whether BB0666 is a MurNac-LAA, we attempted to analyze its enzymatic activity. However, the recombinant BB0666 formed inclusion bodies that could not be renatured. Thus, such biochemical analysis cannot be performed. A similar phenotype was observed in the *E. coli* AmiB (Heidrich *et al*., 2001).

Acknowledgments

We thank S. Samuels for providing the shuttle vectors, J. Radolf for providing the mutant gpf gene and W. Zhang for measuring the fluorescence of GFP. This research was supported by the United States Public Health Service AI073354, AI078958, and the American Heart Association 0735236N to C.L., and AI29743 to N.W.C.

References

Aldridge P, Hughes KT. Regulation of flagellar assembly. Curr Opin Microbiol 2002;5:160–165. [PubMed: 11934612]

Aldridge PD, Karlinsey JE, Aldridge C, Birchall C, Thompson D, Yagasaki J, Hughes KT. The flagellar-specific transcription factor, sigma28, is the Type III secretion chaperone for the flagellar-specific anti-sigma28 factor FlgM. Gene Dev 2006;20:2315–2326. [PubMed: 16912280]

Barak I, Wilkinson AJ. Division site recognition in *Escherichia coli and Bacillus subtilis*. FEMS Microbiol Rev 2007;31:311–326. [PubMed: 17326815]

Bernhardt TG, de Boer PA. The *Escherichia coli* amidase AmiC is a periplasmic septal ring component exported via the twin-arginine transport pathway. Mol Microbiol 2003;48:1171–1182. [PubMed: 12787347]

Blackman SA, Smith TJ, Foster SJ. The role of autolysins during vegetative growth of *Bacillus subtilis* 168. Microbiology 1998;144:73–82. [PubMed: 9537764]

Bono JL, Elias AF, Kupko JJ III, Stevenson B, Tilly K, Rosa P. Efficient targeted mutagenesis in *Borrelia burgdorferi*. J Bacteriol 2000;182:2445–2452. [PubMed: 10762244]

Carroll JA, Stewart PE, Rosa P, Elias AF, Garon CF. An enhanced GFP reporter system to monitor gene expression in *Borrelia burgdorferi*. Microbiology 2003;149:1819–1828. [PubMed: 12855733]

Charon NW, Goldstein SF. Genetics of motility and chemotaxis of a fascinating group of bacteria: the spirochetes. Annu Rev Genet 2002;36:47–73. [PubMed: 12429686]

Eggers CH, Caimano MJ, Clawson ML, Miller WG, Samuels DS, Radolf JD. Identification of loci critical for replication and compatibility of a *Borrelia burgdorferi* cp32 plasmid and use of a cp32-based shuttle vector for the expression of fluorescent reporters in the Lyme disease spirochaete. Mol Microbiol 2002;43:281–295. [PubMed: 11985709]

Eggers CH, Caimano MJ, Radolf JD. Sigma factor selectivity in *Borrelia burgdorferi*: RpoS recognition of the *ospE/ospF/elp* promoters is dependent on the sequence of the −10 region. Mol Microbiol 2006;59:1859–1875. [PubMed: 16553889]

Frank KL, Bundle SF, Kresge ME, Eggers CH, Samuels DS. *aadA* confers streptomycin resistance in *Borrelia burgdorferi*. J Bacteriol 2003;185:6723–6727. [PubMed: 14594849]

Fraser CM, Casjens S, Huang WM, et al. Genomic sequence of a Lyme disease spirochaete, *Borrelia burgdorferi*. Nature 1997;390:580–586. [PubMed: 9403685]

Fraser CM, Norris SJ, Weinstock GM, et al. Complete genome sequence of *Treponema pallidum*, the syphilis spirochete. Science 1998;281:375–388. [PubMed: 9665876]

Ge Y, Charon NW. An unexpected *flaA* homolog is present and expressed in *Borrelia burgdorferi*. J Bacteriol 1997a;179:552–556. [PubMed: 8990312]

Ge Y, Charon NW. Molecular characterization of a flagellar/chemotaxis operon in the spirochete *Borrelia burgdorferi*. FEMS Microbiol Lett 1997b;153:425–431. [PubMed: 9271872]

Ge Y, Old IG, Girons IS, Charon NW. The *flgK* motility operon of *Borrelia burgdorferi* is initiated by a sigma70-like promoter. Microbiology 1997a;143:1681–1690. [PubMed: 9168617]

Ge Y, Old IG, Saint GI, Charon NW. Molecular characterization of a large *Borrelia burgdorferi* motility operon which is initiated by a consensus sigma70 promoter. J Bacteriol 1997b;179:2289–2299. [PubMed: 9079915]

Heidrich C, Templin MF, Ursinus A, Merdanovic M, Berger J, Schwarz H, de Pedro MA, Holtje JV. Involvement of *N*-acetylmuramyl-L-alanine amidases in cell separation and antibiotic-induced autolysis of *Escherichia coli*. Mol Microbiol 2001;41:167–178. [PubMed: 11454209]

Heidrich C, Ursinus A, Berger J, Schwarz H, Holtje JV. Effects of multiple deletions of murein hydrolases on viability, septum cleavage, and sensitivity to large toxic molecules in *Escherichia coli*. J Bacteriol 2002;184:6093–6099. [PubMed: 12399477]

Holtje JV, Heidrich C. Enzymology of elongation and constriction of the murein sacculus of *Escherichia coli*. Biochimie 2001;83:103–108. [PubMed: 11254982]

Hughes KT, Mathee K. The anti-sigma factors. Annu Rev Microbiol 1998;52:231–286. [PubMed: 9891799]

Hughes KT, Gillen KL, Semon MJ, Karlinsey JE. Sensing structural intermediates in bacterial flagellar assembly by export of a negative regulator. Science 1993;262:1277–1280. [PubMed: 8235660]

Kajimura J, Fujiwara T, Yamada S, Suzawa Y, Nishida T, Oyamada Y, Hayashi I, Yamagishi J, Komatsuzawa H, Sugai M. Identification and molecular characterization of an *N*-acetylmuramyl-L-alanine amidase Sle1 involved in cell separation of *Staphylococcus aureus*. Mol Microbiol 2005;58:1087–1101. [PubMed: 16262792]

Kurtenbach K, Hanincova K, Tsao JI, Margos G, Fish D, Ogden NH. Fundamental processes in the evolutionary ecology of Lyme borreliosis. Nat Rev Microbiol 2006;4:660–669. [PubMed: 16894341]

Li C, Motaleb A, Sal M, Goldstein SF, Charon NW. Spirochete periplasmic flagella and motility. J Mol Microb Biotech 2000;2:345–354.

Li C, Bakker RG, Motaleb MA, Sartakova ML, Cabello FC, Charon NW. Asymmetrical flagellar rotation in *Borrelia burgdorferi* nonchemotactic mutants. P Natl Acad Sci USA 2002;99:6169–6174.

Limberger RJ. The periplasmic flagellum of spirochetes. J Mol Microb Biotech 2004;7:30–40.

Lock RL, Harry EJ. Cell-division inhibitors: new insights for future antibiotics. Nat Rev Drug Discov 2008;7:324–338. [PubMed: 18323848]

Lutkenhaus J. Assembly dynamics of the bacterial MinCDE system and spatial regulation of the Z ring. Annu Rev Biochem 2007;76:539–562. [PubMed: 17328675]

Margolin W. Bacterial division: another way to box in the ring. Curr Biol 2006;16:R881–R884. [PubMed: 17055971]

Mishima M, Shida T, Yabuki K, Kato K, Sekiguchi J, Kojima C. Solution structure of the peptidoglycan binding domain of *Bacillus subtilis* cell wall lytic enzyme CwlC: characterization of the sporulation-related repeats by NMR. Biochemistry 2005;44:10153–10163. [PubMed: 16042392]

Motaleb MA, Corum L, Bono JL, Elias AF, Rosa P, Samuels DS, Charon NW. *Borrelia burgdorferi* periplasmic flagella have both skeletal and motility functions. P Natl Acad Sci USA 2000;97:10899–10904.

Motaleb MA, Sal MS, Charon NW. The decrease in FlaA observed in a *flaB* mutant of *Borrelia burgdorferi* occurs posttranscriptionally. J Bacteriol 2004;186:3703–3711. [PubMed: 15175283]

Paster BJ, Dewhirst FE. Phylogenetic foundation of spirochetes. J Mol Microb Biotech 2000;2:341–344.

Powell AJ, Liu ZJ, Nicholas RA, Davies C. Crystal structures of the lytic transglycosylase MltA from *N. gonorrhoeae* and *E. coli*: insights into interdomain movements and substrate binding. J Mol Biol 2006;359:122–136. [PubMed: 16618494]

Ren SX, Fu G, Jiang XG, et al. Unique physiological and pathogenic features of *Leptospira interrogans* revealed by whole-genome sequencing. Nature 2003;422:888–893. [PubMed: 12712204]

Rice KC, Bayles KW. Death's toolbox: examining the molecular components of bacterial programmed cell death. Mol Microbiol 2003;50:729–738. [PubMed: 14617136]

Rosa PA, Tilly K, Stewart PE. The burgeoning molecular genetics of the Lyme disease spirochaete. Nat Rev Microbiol 2005;3:129–143. [PubMed: 15685224]

Sal MS, Li C, Motalab MA, Shibata S, Aizawa S, Charon NW. *Borrelia burgdorferi* uniquely regulates its motility genes and has an intricate flagellar hook-basal body structure. J Bacteriol 2008;190:1912–1921. [PubMed: 18192386]

Samuels DS. Electrotransformation of the spirochete *Borrelia burgdorferi*. Methods Mol Biol 1995;47:253–259. [PubMed: 7550741]

Serizawa M, Yamamoto H, Yamaguchi H, Fujita Y, Kobayashi K, Ogasawara N, Sekiguchi J. Systematic analysis of SigD-regulated genes in *Bacillus subtilis* by DNA microarray and Northern blotting analyses. Gene 2004;329:125–136. [PubMed: 15033535]

Seshadri R, Myers GS, Tettelin H, et al. Comparison of the genome of the oral pathogen *Treponema denticola* with other spirochete genomes. P Natl Acad Sci USA 2004;101:5646–5651.

Shida T, Hattori H, Ise F, Sekiguchi J. Mutational analysis of catalytic sites of the cell wall lytic *N*-acetylmuramoyl-L-alanine amidases CwlC and CwlV. J Biol Chem 2001;276:28140–28146. [PubMed: 11375403]

Steere AC. Lyme disease. New Engl J Med 2001;345:115–125. [PubMed: 11450660]

Tomioka S, Nikaido T, Miyakawa T, Matsuhashi M. Mutation of the *N*-acetylmuramyl-L-alanine amidase gene of *Escherichia coli* K-12. J Bacteriol 1983;156:463–465. [PubMed: 6137479]

van Asselt EJ, Thunnissen AM, Dijkstra BW. High resolution crystal structures of the *Escherichia coli* lytic transglycosylase Slt70 and its complex with a peptidoglycan fragment. J Mol Biol 1999;291:877–898. [PubMed: 10452894]

Vollmer W, Joris B, Charlier P, Foster S. Bacterial peptidoglycan (murein) hydrolases. FEMS Microbiol Rev 2008;32:259–286. [PubMed: 18266855]

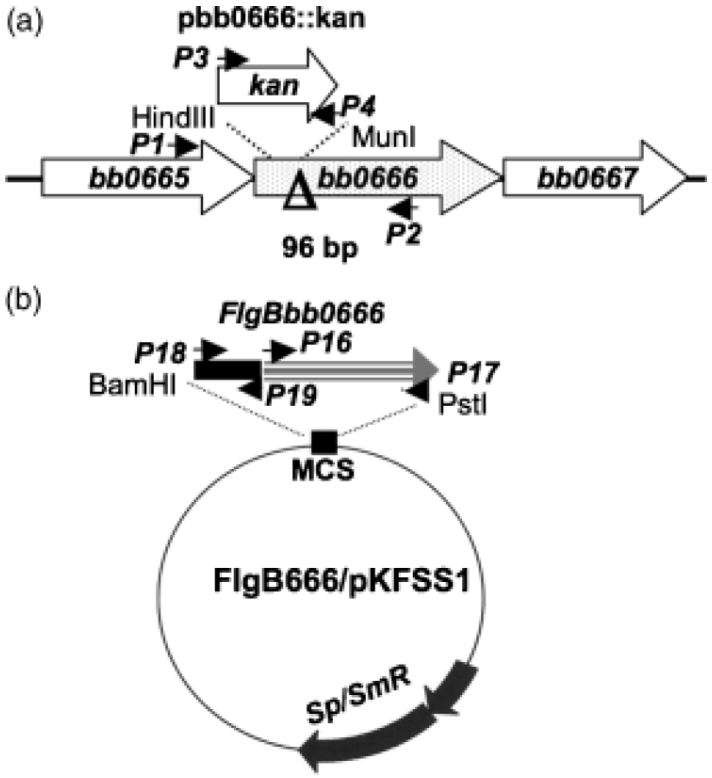

Fig. 1.

Constructing plasmids for the inactivation of *bb0666* and the complementation of Δ*BBB066*. (a) The plasmid pbb0666::kan was used to inactivate *bb0666*. (b) The plasmid FlgB666/pKFSS1 was used to complement Δ*bb0666*. Arrows indicate the relative positions of the primers used for constructing these plasmids. The sequences of these primers are listed in Table 1. The symbol `Δ'shows that a 96-bp HindIII/MunI fragment within *bb0666* was deleted and replaced with the *kan* cassette.

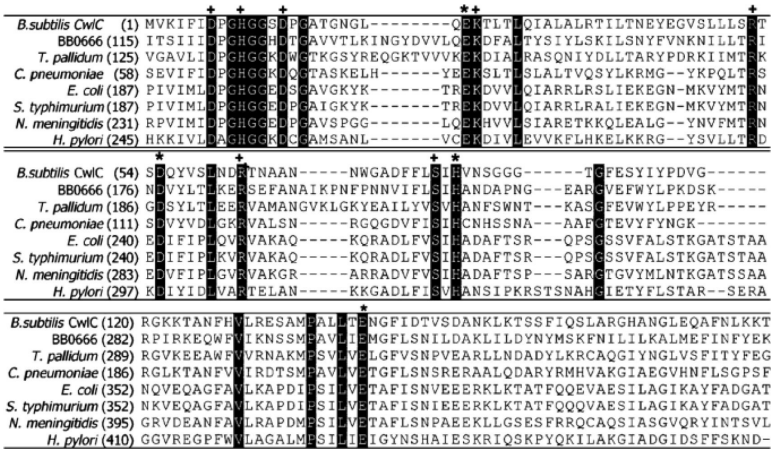

Fig. 2.

Multiple-sequence alignment of the catalytic domains of amidases. Residues with 100% identity are shaded in black. GenBank accession numbers for the aligned sequences are as follows: *Bacillus subtilis* CwlC (BAA03500), *Borrelia burgdorferi* BB0666 (NP_212800), *Treponema pallidum* AmiA (NP_218687), *Chlamydia pneumoniae* AmiA (NP_224617), *Escherichia coli* AmiB (NP_290799), *Salmonella typhimurium* AmiB (NP_463219), *Neisseria meningitidis* AmiC (AF194079) and *Helicobacter pylori* AmiA (NP_207565). The residues labeled with * and+have been studied by amino acid substitutions in CwlC. *Essential residues for the catalytic activity of CwlC (Shida *et al*., 2001). The alignments were performed using the program ALIGNX (Invitrogen).

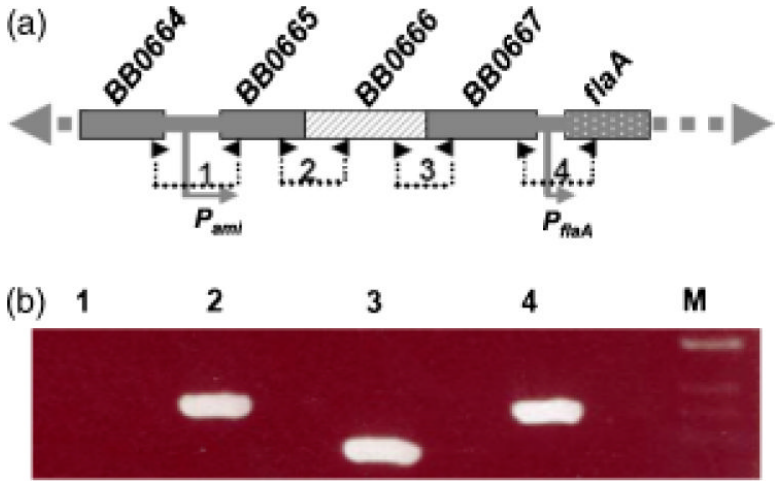

Fig. 3.

Characterization of the pami operon. (a) The diagram showing the genes upstream of the *flaA* operon. The numbers and small arrows show the primers used for RT-PCR analysis. The relative positions of the promoters P_{ami} and P_{flaA} are labeled. (b) RT-PCR analysis. The numbered RT-PCR products were correspondingly produced by the primers labeled in (a). The sequences of these primers are described in Table 1. M, 1-kb DNA ladder.

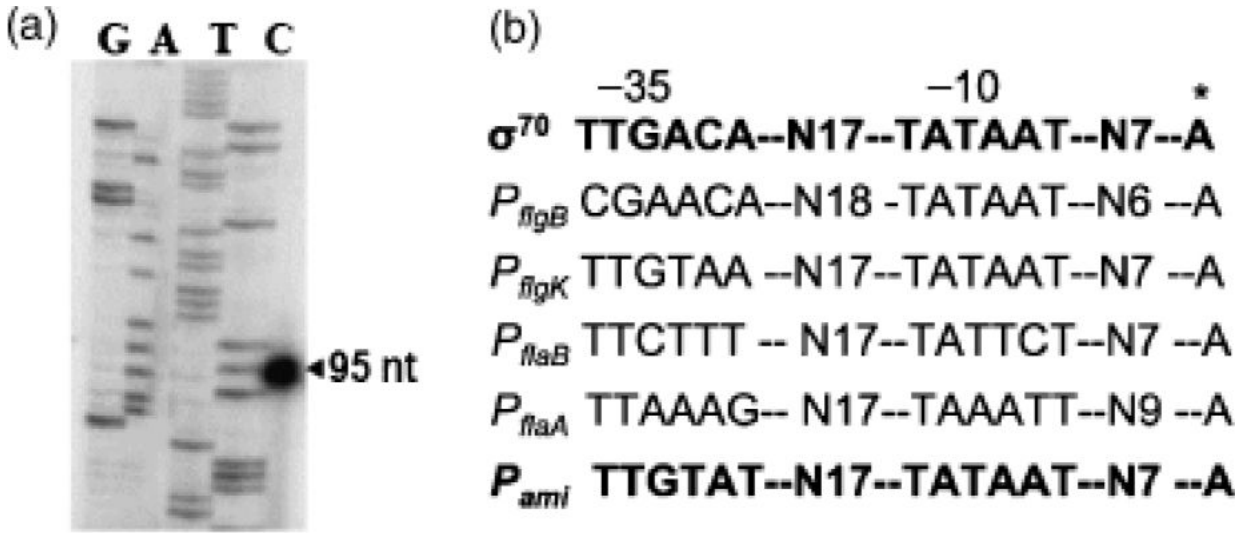

Fig. 4.

The *pami* operon is initiated by a σ^{70}-like promoter, P_{ami}. (a) Primer extension assay. The DNA ladder was generated with a DNA-sequencing reaction using *Borrelia burgdorferi flaA* gene as a template. The number is the size of the cDNA product generated from the primer extension assay. (b) Comparison of the P_{ami} sequence with other σ^{70}-like promoters identified in *Escherichia coli* and *B. burgdorferi* (Ge *et al*., 1997a, b). The asterisk indicates transcriptional initiation sites.

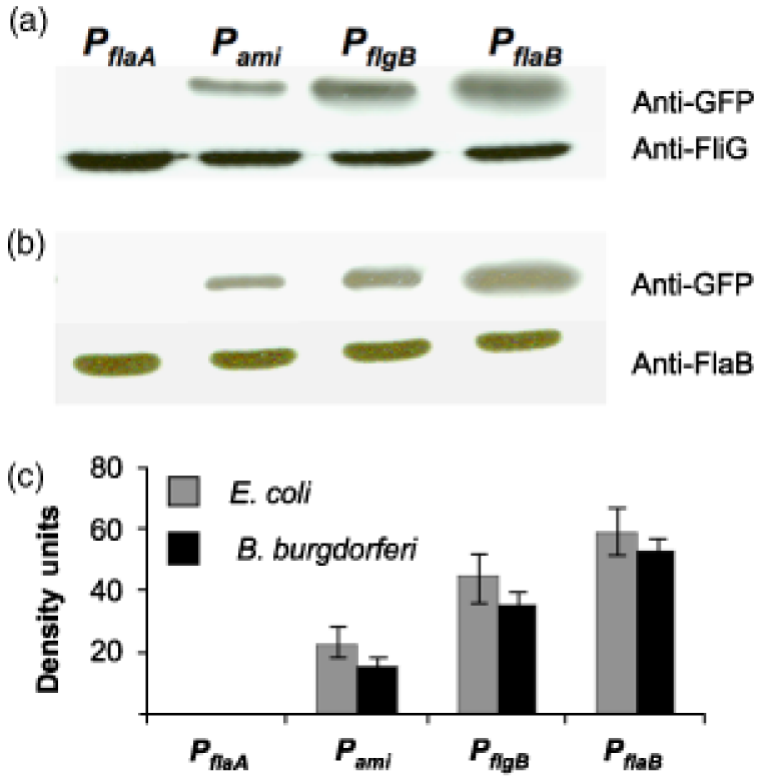

Fig. 5.

Transcriptional analysis of P_{flaA}, P_{ami}, P_{flgB} and P_{flaB} promoters using *gfp* as a reporter. The levels of GFP in (a) *Escherichia coli* and (b) *Borrelia burgdorferi* were detected by Western blot analysis. Approximately 10 μg of whole cell lysates were run by SDS-PAGE. The flagella motor switch complex protein, FliG, and the flagella filament protein, FlaB, were used as internal controls in *E. coli* and *B. burgdorferi*, respectively. The monoclonal antibodies against GFP and FlaB, and polyclonal antiserum against *E. coli* FliG, were used. (c) Quantitative Western blot analysis of GFP levels in *E. coli* and *B. burgdorferi*. Protein density was determined by FluorChem spot densitometry (Bio-Rad). Data were expressed as mean of density unit±SD of the mean from three independent experiments.

Fig. 6.

Characterization of Δ*bb0666* and the complemented strain Δ*bb0666*$^{+}$ by Western blot analysis. Approximately 10 μg of whole cell lysates were run by SDS-PAGE, and the polyclonal antiserum against *Borrelia burgdorferi* BB0666 was used for Western blots. WT, wild type.

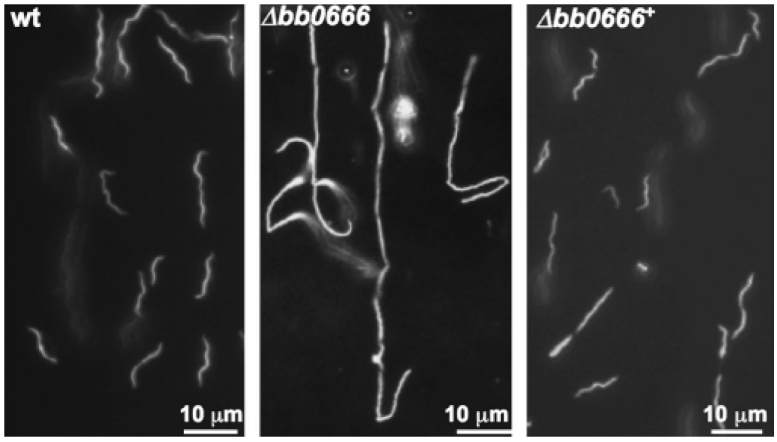

Fig. 7.

Phenotypic analysis of Δ*bb0666*. The middle stationary phase cultures of the wild type, Δ*bb0666* and the complemented strain Δ*bb0666*$^{+}$ were observed by dark-field microscopy. At least 20 fields were examined for each strain.

Table 1

Oligonucelotide primers used in this study

Primer	Description	Sequences
P1	*bb0666* (F), inactivation	5′-TACAGCTTGGAGGTTTTGACG-3′
P2	*bb0666* (R), inactivation	5′-TGCAAATTCCGACCGTTC-3′
P3	*kan* (F), inactivation	5′-AAGCTTTAATACCCGAGCTTCAAG-3′
P4	*kan* (R), inactivation	5′-CAATTGTCAAGTCAGCGTAATGCT-3′
P5	*bb0666* (F), expression	5′-GGATCCATTTTGTTTTCATATTTAAGC-3′
P6	*bb0666* (R), expression	5′-CTGCAGCATTAAAGCTTTAAGTATTAG-3′
P7	*bb0664* (F), RT-PCR	5′-ATAAAGTCATTTTCTGAG-3′
P8	*bb0665* (R), RT-PCR	5′-AAATTTTTGTTCCTCTGC-3′
P9	*bb0665* (F), RT-PCR	5′-TTTTTGTTGGAAATGGCG-3′
P10	*bb0666* (R), RT-PCR	5′-CTTCAAATATCCCTTATC-3′
P11	*bb0666* (F), RT-PCR	5′-AACAGCAGTATGCCTGCT-3′
P12	*bb0667* (R), RT-PCR	5′-AACAAAAAGCTTACTGCC-3′
P13	*bb0667* (F), RT-PCR	5′-TAAGGTCAATCTTTTTGC-3′
P14	*bb0668* (R), RT-PCR	5′-TAGTTGAACTTGGATCTC-3′
P15	*bb0665* (R), primer extension	5′-AAAGAAGATTTTTGTG-3′
P16	*bb0666* (F), complementation	5′-CATATGCCATTGAGCTTTGGGAAAATG-3′
p17	*bb0666* (R), complementation	5′-CTGCAGAGCACCCTAATCATATGC TC-3′
P18	*flgBp* (F), complementation	5′-GGATCCTAATACCCGAGCTTCAAG-3′
P19	*flgBp* (R), complementation	5′-CATATGACCTCCCTCATTTAAAATTGC-3′
P20	*gfp* (F), expressing GFP	5′-GGATCCAAGAAGGAGATATACATATG-3′
P21	*gfp* (R), expressing GFP	5′-CTGCAGTTTGTATAGTTCATCCATGCC-3′
P22	*flaAp* (F), *flaA* promoter	5′-CTGCAGTGCGCTTTAACTATCCTG-3′
P23	*flaAp* (R), *flaA* promoter	5′-GGATCCCATGTAAACCAACTCCTT-3′
P24	*pami* (F), *pami* promoter	5′-CTGCAGAAAGTCATTTTCTGAGTC-3′
P25	*pami* (R), *pami* promoter	5′-GGATCCAAATTACTTTTAAAATCC-3′
P26	*flgBp* (F), *flgB* promoter	5′-CTGCAGTAATACCCGAGCTTCAAG-3′
P27	*flgBp* (R), *flgB* promoter	5′-GGATCCACCTCCCTCATTTAAAATTGC-3′
P28	*flaBp* (F), *flaB* promoter	5′-CTGCAGTGTCTGTCGCCTCTTGTGG-3′
P29	*flaBp* (R), *flaB* promoter	5′-GGATCCATATCATCCCTCCATGAT-3′
P30	*aadA* (F), pKFSS1	5′-TATCAGAGGTAGTTGGCGTC-3′
P31	*aadA* (R), pKFSS1	5′-TGTCTAGCTTCAAGTATGACG-3′

F, forward; R, reverse. The underlined sequences are engineered restriction enzymes for cloning.

Table 2

Percentile of unseparated cells in the wild type and the Δ*bb0666* mutant

	WT			Δbb0666		
	2*	3–6	>6	2	3–6	>6
Early log-phase (<10^5)	10–20%	<1%	NA	30–40%	<5%	<1%
Middle log-phase (<10^7)	10–20%	<1%	NA	40–50%	20–30%	<10%
Stationary phase (>10^8)	20–30%	<2%	NA	5–10%	50–60%	<20%

WT, wild type.

*Number of cells per chain. The remaining percentages are attributed to single cell per chain.